Research on Full-Field Deformation Testing of 3D Printed Bridges Based on DIC Technology

Chenyang Su[1], Huiru Huang[1*], Xia Guo[2]

[1]*Beijing City University, Beijing , 101309; China*
[2]*Institute of Analysis and Testing, Beijing Academy of Science and Technology（Beijing Center for Physical & Chemical Analysis）, Beijing, 100089, China*
[*]*Corresponding author:huanghuiru@163.com*

Abstract: *With the acceleration of urbanization, traditional bridge construction methods face dual challenges of efficiency and cost. 3D printing technology offers an innovative solution for bridge engineering. This study combines Digital Image Correlation (DIC) technology with numerical simulation methods to systematically analyze the full-field deformation characteristics of double-arch and four-arch 3D printed bridges under different load conditions. By comparing physical loading tests with finite element simulations, this research reveals the influence patterns of aperture geometric features on structural stiffness, stress distribution, and bearing capacity.*

Keywords: *DIC technology; 3D printed bridges; full-field deformation testing; numerical simulation*

Introduction

As a core component of transportation infrastructure, the safety and durability of bridges directly affect urban development. Traditional bridge construction relies on complex formwork and high labor costs, whereas 3D printing technology, with advantages such as high design freedom, low material waste, and short construction cycles, has gradually become a research focus in bridge engineering. However, the structural performance of 3D printed bridges still requires in-depth verification. Digital Image Correlation (DIC) technology, as a non-contact full-field optical measurement method, can acquire high-precision strain and deformation data by tracking surface speckle displacement, providing a new approach for structural health monitoring. This study focuses on utilizing DIC technology to perform full-field deformation testing on 3D printed bridges with different structures, aiming to reveal the mechanical response patterns of the structures under various loads, identify weak points, and propose optimization strategies to promote the engineering application of 3D printed bridges.

1. Experimental Plan and Methods

1.1 Bridge Model Design and Fabrication

The study selected two typical arch bridge models: Bridge 1 (double-arch) and Bridge 2 (four-arch), which were printed using fused deposition modeling (FDM) technology with PLA resin as the material. The model dimensions were 200 × 90 × 60 mm, with the main arch rings shaped as circular arcs, having a rise-to-span ratio of 1:6.66 and a width-to-span ratio of 1:4. The models were created and optimized for printing paths using 3Dmax software to ensure geometric accuracy and consistency.
To collect experimental data, black matte paint was sprayed on the bridge surfaces to form speckle patterns.
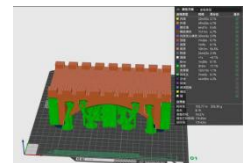

Figure 1 Bridge 1   Figure 2 Bridge 2   Figure 3 Printing scheme of Bridge 1
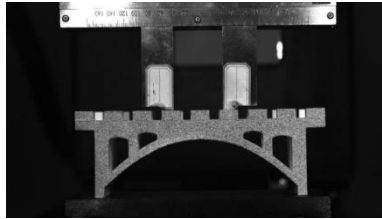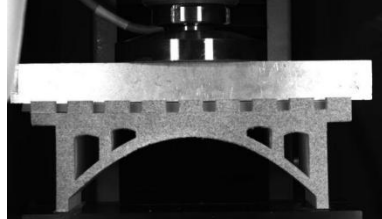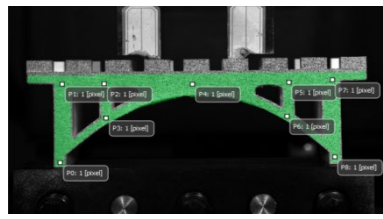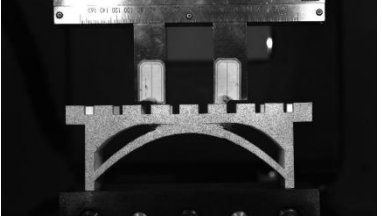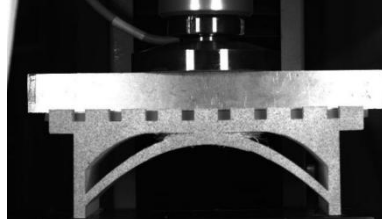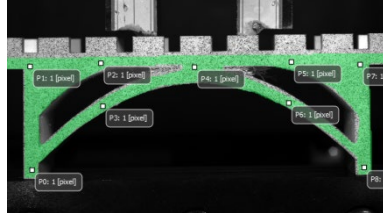
1.2 Physical Loading Test

The physical loading test was conducted using a universal testing machine to apply various types of loads, while a non-contact full-field strain measurement device simultaneously recorded deformation images, strain, and displacement data of the bridge under each load level. The deformation of the bridge during loading was observed, with particular attention paid to stress concentration and deformation trends around the openings[1].

The physical tests on the 3D printed bridges mainly covered the following loading conditions:

1)Symmetrical double concentrated load: applying 0–150 N loads on both sides of the bridge deck centerline;

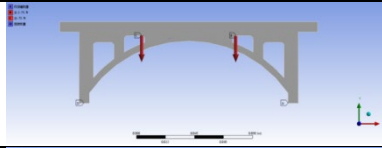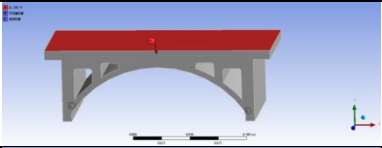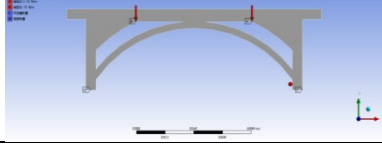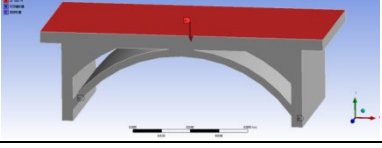2)Uniformly distributed load: applying a continuous distributed load of 0–200 N on the bridge deck;

Table 1 Physical loading test charts

Test Schee / Bridge Type	Apply continuous concentrated forces (0–150 N) at two symmetrical positions on the bridge deck	Apply continuous uniformly distributed loads (0–300 N) on the bridge deck	Measurement Point Selection Diagram
Bridge 1			
Bridge 2			

1.3 Numerical Simulation Calculation

The finite element model of the bridge was constructed, with material parameters set based on the measured values of PLA resin. The bridge boundary conditions involved one end fixed support and the other end compression-only support. The boundary conditions simulated the actual support state (one end fixed, the other end compression-only), and the load types matched those of the physical tests. The model reliability was verified and the errors were quantified by comparing simulation results with experimental data.

Table 2 Static Structural Diagrams of the Bridge

Test Plan / Bridge Types	Apply continuous concentrated forces (0–150 N) at two symmetrical positions on the bridge deck	Apply continuous uniformly distributed load (0–300 N) on the bridge deck
Bridge 1		
Bridge 2		

2. Data Analysis and Results

2.1 Physical Loading Test

Select measurement points covering key stress regions, and record and analyze their vertical displacement changes in relation to the magnitude of external loads by monitoring the deformation data at these points, thereby intuitively reflecting the overall stiffness and load-bearing capacity of the bridge.

Table 3 Vertical Deformation Charts of Measurement Points Throughout the Entire Physical Loading Test

Test Plan / Bridge Types	Apply continuous concentrated loads (0–150N) at two symmetrical positions on the bridge deck	Apply continuous uniformly distributed loads (0–200N) on the bridge deck
Bridge 1		
Bridge 2		

According to the chart, the vertical deformation of measurement points (P0–P8) at different positions on the bridge shows varying trends as the total load increases. Among them, P4 exhibits the most significant decrease in deformation with increasing load, while P0, P1, P7, and P8 show minimal vertical deformation, remaining nearly unchanged. This indicates that, due to structural heterogeneity and varying stress distribution across different parts of the bridge, the response of each point to the load differs. Moreover, under identical loading conditions, the vertical deformation at corresponding measurement points is noticeably smaller on Bridge 1 than on Bridge 2. When two 75N concentrated loads are applied symmetrically on the bridge deck, the maximum deformation occurs at the arch crown area (P4), with Bridge 1 showing a deformation of –0.62 mm and Bridge 2 showing –1.00 mm, indicating that Bridge 1 possesses superior load-bearing capacity compared to Bridge 2[2].

2.2 Numerical Simulation

Loading tests of the same type, magnitude, and location as those in the physical experiments were conducted. Numerical simulation and analysis of the bridge structure were performed using general-purpose finite element software.

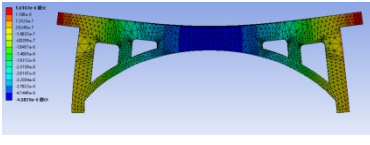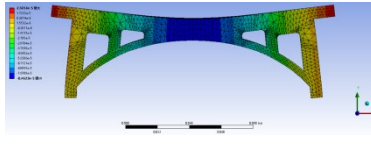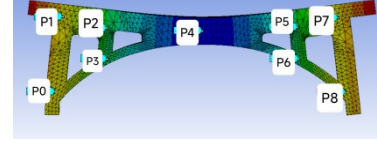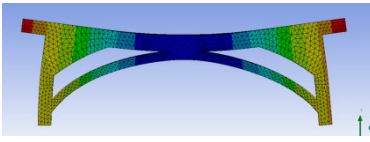*Table 4 Deformation Contour of Bridge and Diagram of Measurement Point Locations*
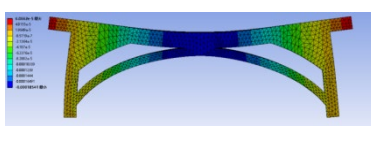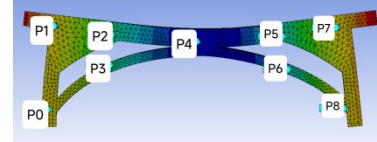
Test Plan / Bridge Type	Continuous concentrated forces applied at two symmetrical positions on the bridge deck (0–150 N)	Continuous uniformly distributed load applied on the bridge deck (0–300 N)	Measurement Point Locations on the Bridge Deck
Bridge 1			
Bridge 2			

Table 5 Vertical Deformation of Measurement Points in Numerical Simulation
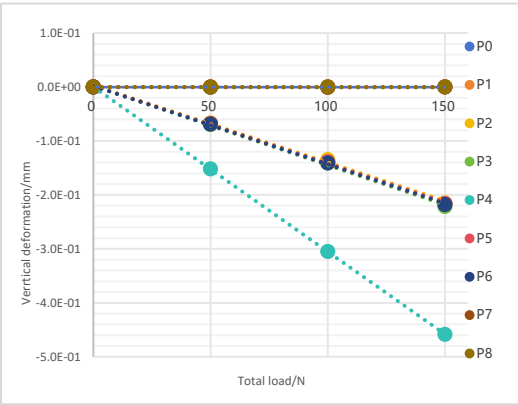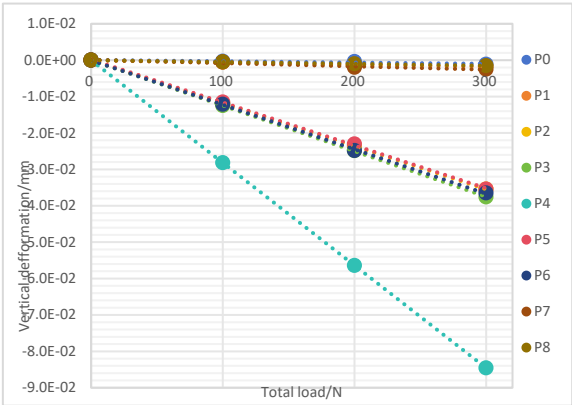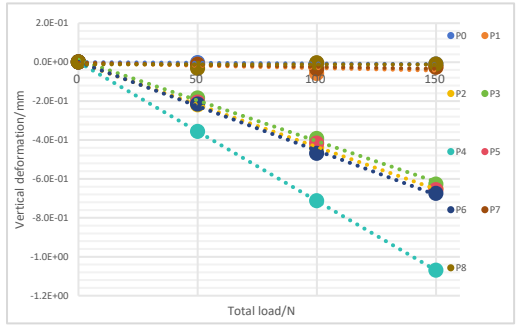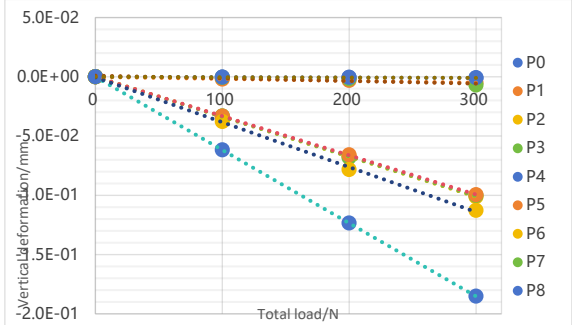
Test Plan / Bridge Type	Continuous concentrated forces applied at two symmetrical positions on the bridge deck (0–150 N)	Continuous uniformly distributed load applied on the bridge deck (0–300 N)
Bridge 1		
Bridge 2		

The load-bearing deformation diagram of the bridge shows an uneven distribution of deformation. The arch crown exhibits the largest negative vertical deformation, while the sides of the bridge deck show the largest positive vertical deformation in the vertical direction. Deformation in other areas is relatively minor. Under identical loading conditions, the vertical deformation at the same measurement points on Bridge 1 is significantly smaller than that on Bridge 2, indicating that Bridge 1 has superior load-bearing capacity[3].

2.3 Comparison and Analysis of Physical Load Test and Numerical Simulation Calculation

Relevant result data from bridge deck measurement points P2, P4, and P5 were primarily extracted. Measurement points from the physical load test are denoted as P2, P4, and P5, while those from the numerical simulation are denoted as p2, p4, and p5.

Table 6 Comparison and Analysis of Experimental and Simulation Results

Test Scheme / Bridge Type	Continuous concentrated load (0–150 N) applied at two symmetrical positions on the bridge deck	Continuous uniformly distributed load (0–200 N) applied on the bridge deck
Bridge 1		
Bridge 2		

Under both loading conditions, the displacement variation trends of the physical test measurement points for both bridges show a high degree of consistency with the numerical simulation results, with measurement point P4 at mid-span exhibiting the maximum deformation in each case. By comparing the outcomes of the physical loading tests and the numerical simulations, and considering the performance of Bridge 1 (four-arch structure) and Bridge 2 (double-arch structure) under different loading scenarios, the experimental and simulation results are deemed to be consistent.

3. Conclusions and Recommendations

This study, based on Digital Image Correlation (DIC) technology and incorporating both finite element simulation and physical loading tests, systematically analyzed the full-field deformation characteristics of two structurally distinct 3D-printed arch bridges under various loading conditions. The following conclusions were drawn:

3.1 Structural Stiffness and Load-Bearing Capacity

Under multiple loading conditions, the maximum displacement of Bridge 1 was significantly smaller than that of Bridge 2, indicating a noticeable improvement in stiffness. This demonstrates that

the four-hole structure of Bridge 1 is more advantageous than the two-hole structure of Bridge 2 in distributing loads and limiting overall deformation.

3.2 Recommendations for Structural Optimization

Material Enhancement: For high-strain regions near the arch crown, the use of higher-strength materials (such as fiber-reinforced PLA or carbon fiber composites) is recommended to improve tensile strength and flexural modulus, thereby preserving the intended aesthetic design.

3.3 Research Limitations and Future Work

This study did not consider the effects of temperature and long-term creep. Future research should include environmental coupling tests. In addition, the current loading range was limited; future studies should extend to failure loads to reveal failure modes.

References

[1] Chen Yajun, Sun Shengjie, Ji Chunming. Progress in the Application of Three-Dimensional Digital Image Correlation Technology (3D DIC) in Material Deformation Research [J]. Journal of Aeronautical Materials, 2017, 37(04): 90-100.
[2] He Fan, Li Bingtao, Fu Baiyong. Discussion on 3D Printing Technology and Its Application in Highway Bridges [J]. Highway, 2019, 64(02): 105-109.
[3] Han Bing, Wei Xing, Zhang Weiyong, et al. DIC Measurement Technology for Testing the Ultimate Bearing Capacity of Stiffened Plate Girders [J]. China Testing, 2023, 49(08): 47-52.